12.6

Comparison of the down-valley flow for the MAP IOP8 and IOP3 with the numerical laboratory Mesonh model .

Nicole Asencio[1], Joel Stein[1] and Michel Chong[2]

[1] Centre National de Recherches Météorologiques (CNRS and Météo-France), Toulouse, France

[2] Laboratoire d'Aérologie , Toulouse, France

1. INTRODUCTION

Persistent rainy periods and meso-scale south-westerly flow characterize the two MAP IOPs, IOP3 (24 to 27 September 1999) and IOP8 (20 to 21 October 1999). A down-valley flow has been observed inside the major western Alpine valleys (Toce, Ticino, Como valleys) by the DOW radar (Steiner *et al.*2003)(location is pointed out on Fig.1b). This northerly flow was confined over the north-western part of the Po valley in a thin layer of 200-300 meters height for the IOP3. The IOP8 northerly flow widely spread from Alps foothills to far over the Ligurian sea in a deep layer of 1-2km height(Bousquet *et al.*2003).

We use the Mesonh model as a numerical laboratory by performing sensitivity experiments to quantify the respective role of each mechanisms previously identified as a potential cause of this reverse flow: wet or dry drainage flow, blocking upstream the Alps, cold pool inside the Po valley.

2. NUMERICAL SET-UP

The numerical simulations are performed with the anelastic non-hydrostatic meso-scale model Meso-NH (Lafore *et al.*1998). We use 2 nested models: the different horizontal meshes are 10 km (200x160 points) and 2.5 km (362x242 points).

The two simulation domains are shown in Figure 1a. The simulations start the first day of the IOP at 0000

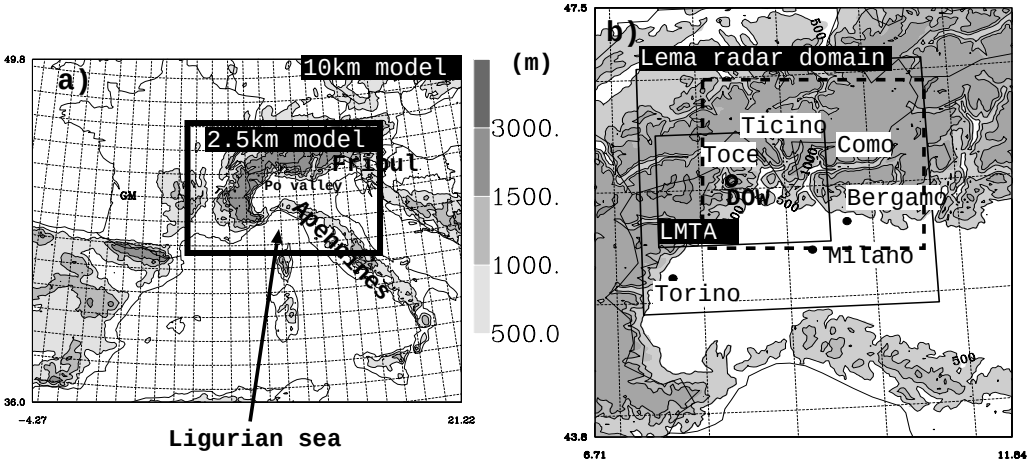

Figure 1: *Nested models domains used in numerical simulation and topographic map. The orography is represented in grey scale (m).(a) The solid line rectangle represents the 2.5km mesh model domain.(b)In a 2.5km model zoom, the solid line rectangles represent the LMTA area and the Lema radar domain, the dashed rectangle localizes the sensitivity area*

UTC and last 54 hours. Different initial conditions and lateral boundary conditions linearly interpolated in time between 6 hourly analyses are tested: the French operational analysis Action de Recherche Petite Et Grande Echelle (ARPEGE), the operationnal ECMWF analysis and the MAP re-analysis performed at ECMWF (Keil and Cardinali

[1] *Corresponding author address*: Nicole Asencio, CNRM, 42 av. Coriolis, 31057 Toulouse Cedex, France. e-mail:nicole.asencio@meteo.fr

2003). The microphysical scheme includes the three water phases with five species of condensed water. For the 10km mesh model, the subgrid-scale convection is parametrized by a mass flux convection scheme (Bechtold *et al.*2001). For the 2.5km mesh model, the convection is explicitly resolved and the convection scheme is switched off.

Sensitivity experiments have been performed by modifying the 2.5km model microphysical scheme i.e. removing the rain evaporation cooling (called **nev experiment**), and removing both the rain evaporation cooling and the cold hydrometeors melting cooling (called **nmt experiment**) over a limited area shown with a dashed rectangle in Fig.1b. The sensitivity experiments start at the beginning of the northerly low-level flow: 0900UTC on 25 September and last 12 hours , 1200UTC on 20 October and last 24 hours.

3. SIMULATIONS VALIDATION

The Mesonh simulations are fully validated with all the available observations data: surface data, Rain product derived from the operational Monte-Lema radar (not shown), the reflectivity and the wind 3D fields derived from the MAP-research ground-based and airborne radars(not shown).

The IOP3 validation has been detailed in the Brig meeting presentation (Asencio *et al.*2003). The same validation protocol has been followed for the IOP8 simulation.

We use the precipitation analysis by Frei and Häller (2001) to validate the different simulations. The initial conditions given by Arpege provides the best distribution of the precipitation over the Po valley and the LMTA area (Lago Maggiore Target Area)Fig.2.

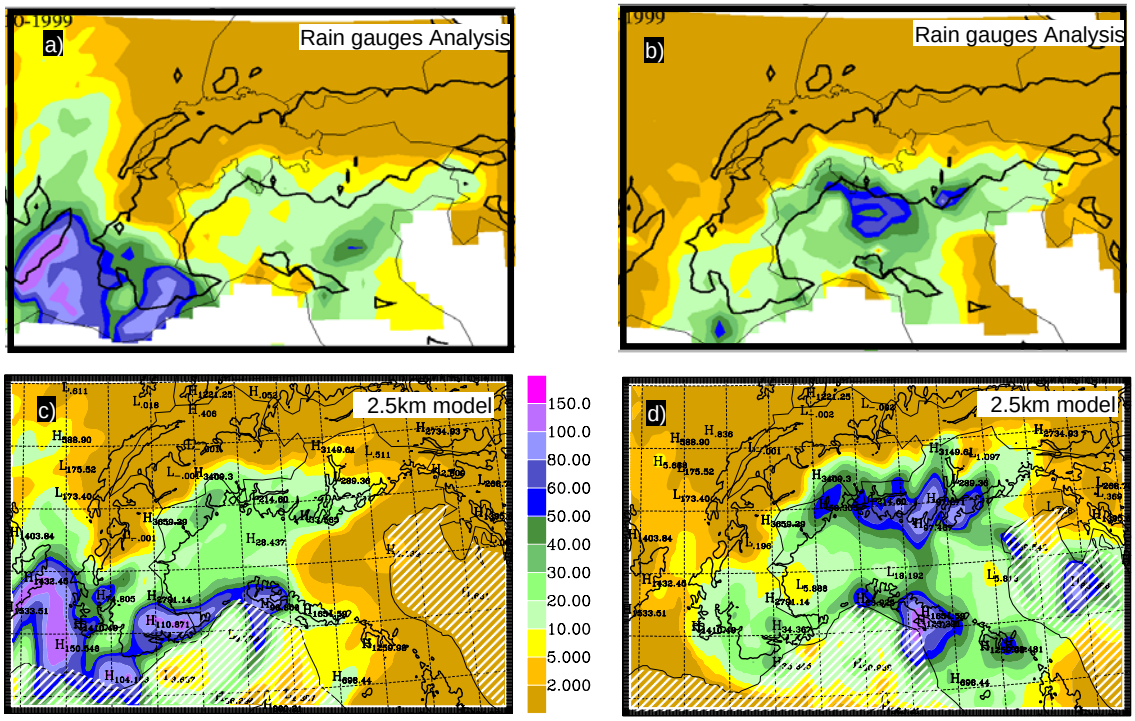

Figure 2: *24 hours accumulated rain (mm) averaged on a 25 km horizontal as deduced from the precipitation analysis by Frei and Häller (2001) for the 20 October (a) and 21 October(b) and from the 2.5km model output for these two dates (c and d). The isoline represents the topography at 800 m ASL. The white dashed areas (c and d) could not be compared to the observations.*

The frontal system evolution is successfully represented in the simulation with a French maxima (a and c) on 20 October and a central Po maxima (b and d) on 21 October. For the first day, the pre-frontal convective systems triggered over Ligurian sea do not pass over the Apennines in the simulation, so the rain maximum is simulated upstream the Apennines (c) but the LMTA weak core precipitation is well represented. For the second day, i.e. frontal passage over the Po valley, the spatial distribution over Northern Italy is close to the rain-gauge analysis but the LMTA core (d) is over-estimated.

The intensity and the temporal evolution Fig.3 focused over LMTA area (rectangle Fig.1b) confirms that simulated precipitation (black curve) begins sooner on pre-frontal period (20 October), strengthens with the front arrival and stops during the evening of the second day with a weak over-estimation.

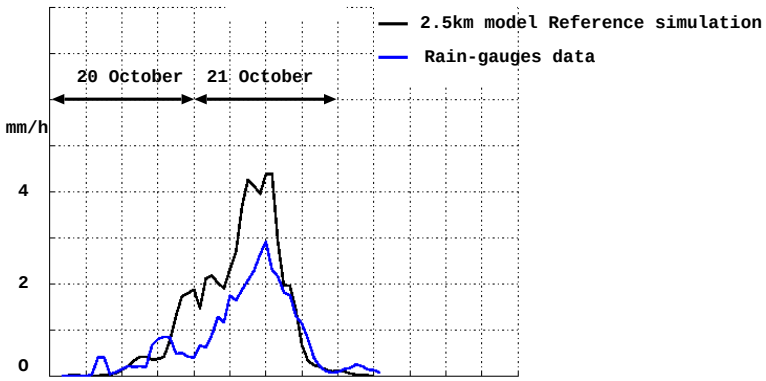

Figure 3: *Time evolution of one hour accumulated rain over Monte-Lema radar area: hourly rain-gauges precipitation (blue) and simulated precipitation (black) interpolated at the rain-gauge locations.*

The western part of the Po valley is invaded by a cold low-level airmass (Fig.4a: 285K at 450 meters ASL) dating back to 16-17 October and continuously fed from the Frioul area by a low-level easterly flow (Bousquet *et al.*2003). This cold pool remains during the two days of the IOP8, it is gradually eroded by the moister and warmer southerly inflow ahead the frontal system (Rotunno and Ferretti 2003) which stops the easterly Frioul feeding. A northerly flow extended from the Alps foothills to far over the Ligurian sea is simulated on 20 October 1999. Its southern limit moves back to Alpine orography when the southerly flow becomes strong enough on 21 October. The outflow of three major valleys (Toce Valley, Ticino Valley and Como Valley), remains stationary (Fig.4b) from 20 to 21 October 1999 until the easterly low-level flow reaches the Alps foothills.

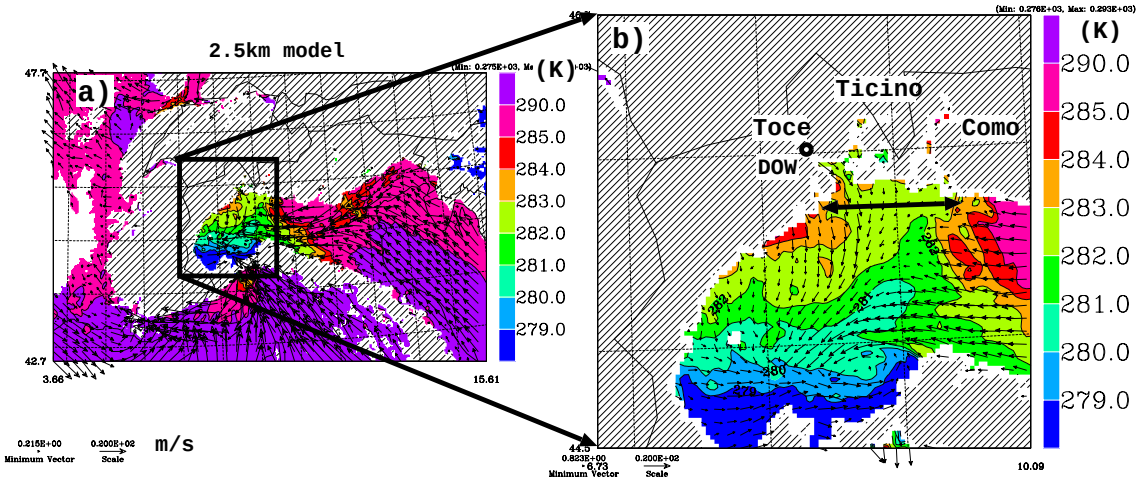

Figure 4: *Potential temperature (K) and vectors wind at 450 meters ASL at 0600 UTC on 21 October 1999. The black segment localizes the vertical cross section of the following figures.*

The observation of Pieve Vergonte at the DOW location in the Toce valley reveals a northerly flow starting on 20 October evening simultaneously to the precipitation and lasting to the end of the 21 October. The Mesonh simulation well represented the observations of this hydrometeorological station (Fig.5 compared to Fig.6 of Steiner *et al.*2003) .

4. ORIGINS OF THE NORTHERLY LOW-LEVEL WIND FOR THE TWO IOPs

The main difference in the meso-scale features for the two IOPs is represented by the IOP8 cold pool in the western part of the Po valley which drives the limit between the easterly low-level jet extension and the northerly low-level flow. For IOP8, two simultaneous mechanisms contribute to the wide extent of the reverse flow: a down-valley

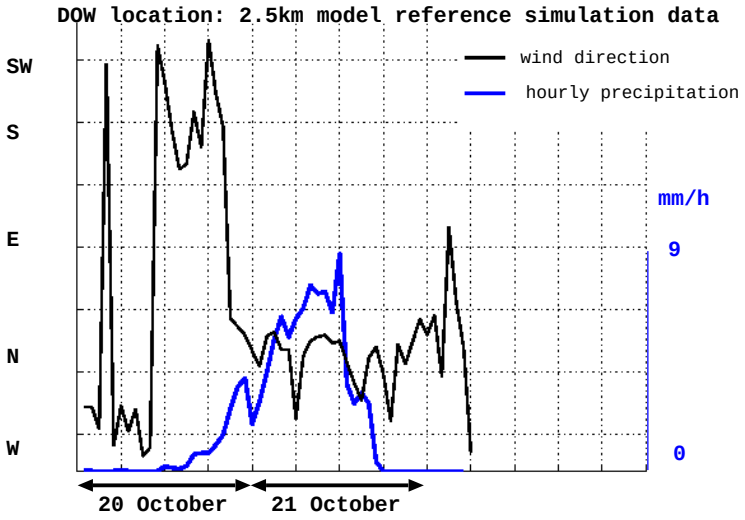

Figure 5: *Time evolution of the wind direction (degrees) and hourly precipitation (mm/h) at DOW location simulated from the 2.5km mesh Mesonh model.*

flow contribution at the foothills of the Toce valley outflow and a blocked low-level easterly flow which follows the concavity shape of the Alps and exits in the Ligurian Sea. During the pre-frontal period this cold air mass protects the foothills of LMTA area from opposite moist and warm flow and so lets the down-valley flow reach the plain. After the front passage, low-level air mass has been warmed by the post-frontal airmass but the easterly low-level intensity flow decreases and could no longer be opposite to persistent down-valley flow. The upper-level flow (above 1500m) passes over this cold pool and more easily passes then over the Alpine orography. Figure 6 shows the thickness of the reverse flow at the major Alpine valleys exit for the IOP8 and IOP3.

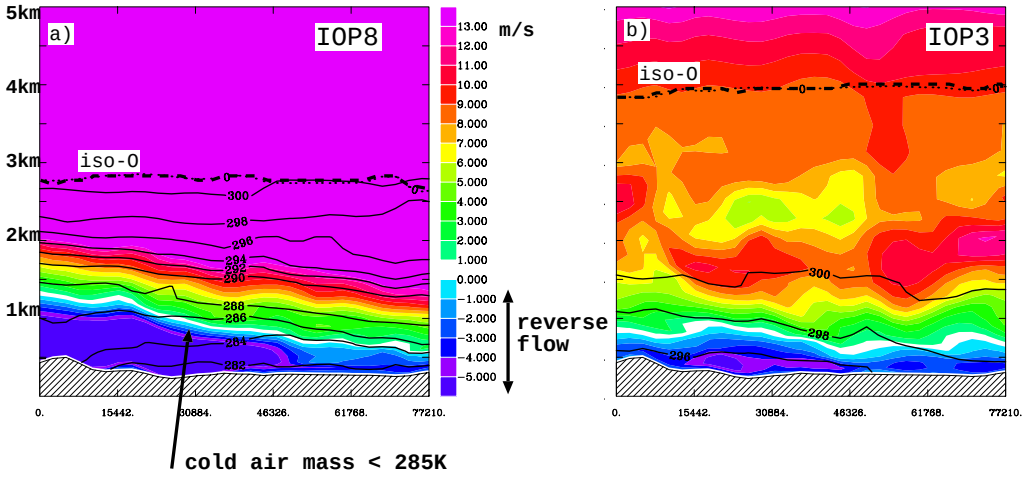

Figure 6: *Cross section of the meridional wind (m s^{-1}) - negative values for northerly direction) at 0600 UTC on 21 October (a) and 1700 UTC (b) on 25 September 1999 at the outflow of the three valleys Toce, Ticino, Como. The potential temperature is represented with heavy lines.*

For both IOPs, the reverse flows are present before the precipitation beginning but their duration are different.

In order to quantify the importance of wet mechanisms to the evolution of the reverse flow plain extension ,we performed different sensitivity experiments by modifying the temperature exchanges inside the micro-physical scheme and specially by removing the cooling associated to the rain evaporation and by removing the cooling associated to the cold hydrometeors melting (graupel,snow). These modifications were applied on a limited geographical area (black

rectangle in Fig.1b) and on a limited period (24 hours at the most) in order to keep the same synoptic environment i.e. the frontal passage. The geographical area was linked to the rainfall location during the northerly flow period upstream a down-valley-oriented direction.

As illustrated in Brig meeting, the reverse outflow of the three valleys (Toce, Ticino, Como valley) is not correlated to the rainfall (black and blue curves in Fig.7): it stops when the precipitation begins, comes back when the precipitation are stationary, vanishes with the intensification of the rain and comes back when the precipitation stops.

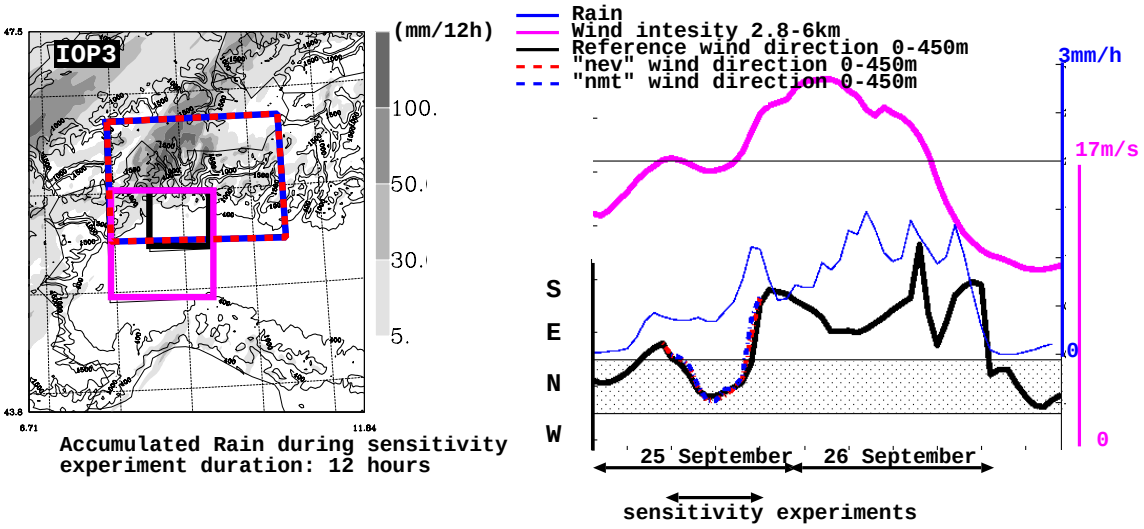

Figure 7: *Temporal evolution for different sensitivity experiments of averaged parameters inside areas: back and dashed curves for the wind direction beneath 450m ASL (degrees), blue curve for hourly accumulated rain (mm h^{-1}), pink curve for the wind intensity (m s^{-1}) between 2.8km and 6km. The same color is used for the average-areas and the curves. The curves represent the different sensitivity experiments and the hashed zone shows Northerly directions.*

A strongly correlation is revealed between the upstream upper-level wind intensity (pink curve) and the northerly low-level flow (black curve). It could be explained by lagrangian trajectories (Gheusi and Stein *et al.*2002) which illustrate (not shown) that the southwesterly upper-level airmass (above 3km) passes over the crest while the low levels are blocked by the orography underneath 1.5km and subside along the slopes contributing to the down-valley flow. The blocked-unblocked shift occurs when the upstream flow is strong enough (greater than 17 m s^{-1}): the upper-level inflow drives the evolution of the reverse low-level flow.

The removing of the cooling (**nev experiment**) associated to the rain evaporation does not modify the reverse flow at the Lakes exit, it only delays of one hours the beginning of the northerly flow (see red dashed curve in Fig.7) for the IOP3.

The supplementary removing of the cooling (**nmt experiment**) associated to the cold hydrometeors melting shows a weak contribution for the IOP3 (see blue dashed curve in Fig.7) where the altitude of the iso 0-level was around 4000 meters (Fig.6). The wet drainage weakly contributes to the IOP3 reverse low-level flow.

During the IOP8, only the Toce valley contributes to the reverse flow at the foothills of the Alps: so we focus the average-area for the low-level IOP8 flow (black rectangle in Fig.8) at the Toce valley outflow. The sensitivity area and the upper-level flow area are the same than the IOP3 ones.

The figure 8 shows that the wind direction (black curve) shifts to northerly direction when the precipitation (blue curve) begins and it remains during all the rainy period. The upstream upper-level wind intensity (pink curve) does not modify the northerly flow.

The removing of the cooling (**nev experiment**) associated to the rain evaporation gives the similar conclusion than the IOP3 one: it only delays of two hours the beginning of the northerly flow (see red dashed curve in Fig.8). But the supplementary removing of the cooling (**nmt experiment**) associated to the cold hydrometeors melting shows a clear vanishing of the reverse flow for the IOP8 (see blue dashed curve in Fig.8) where the altitude of the iso 0-level was varying from 1000m to 3500m either over the plain or over the orography (Fig.6).

In the IOP8 sensitivity **nmt experiment**, the easterly low-level jet reaches the foothills of LMTA at the beginning of the rainy period because the cold low-level air mass has been eroded at the top by the removing-cooling associated to the melting. The small scale features upstream the LMTA area are different: no more cold air-mass and a stronger

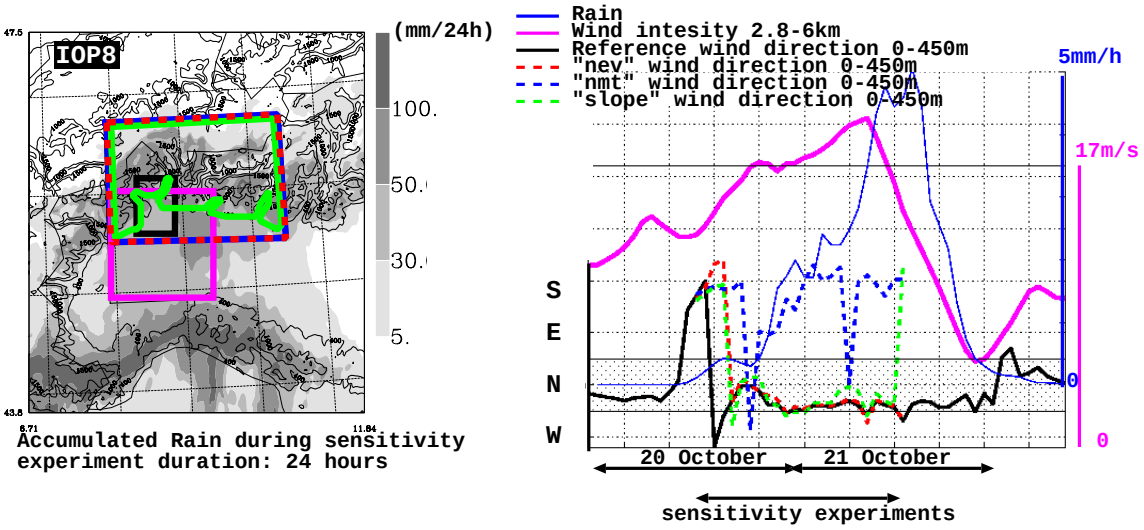

Figure 8: *Temporal evolution for different sensitivity experiments of averaged parameters inside areas: back and dashed curves for the wind direction beneath 450m ASL (degrees), blue curve for hourly accumulated rain (mm h^{-1}), pink curve for the wind intensity (m s^{-1}) between 2.8km and 6km. The same color is used for the average-areas and the curves. The curves represent the different sensitivity experiments and the hashed zone shows Northerly directions.*

easterly jet which is blocked by the Monte Rosa slopes. We could first conclude that the wet effects strongly contribute to the reverse flow extension over the plain.

In order to quantify the specific slopes contribution and to minimize the modifications of the upstream featuresi over the plain, we perform a new sensitivity experiment (**slope experiment**) by applying the same cooling modifications than **nmt experiment** but over a smaller area which includes only the orography points i.e. when altitude is greater than 400 meters (see the green area in Fig.8). The simulated reverse flow (green dashed curve in Fig.8) is quite similar to the reference experiment (black curve) except a delay of two hours for the beginning of the northerly flow period like for the **nev experiment** (red dashed curve). Nevertheless the intensity of this northerly **slope experiment** flow decreases more quickly than the **nev experiment** one (not shown): so it shifts to southwesterly direction at the end of the **slope experiment** when the easterly low-level flow reaches the orography getting strongest than down-valley flow intensity.

In the case of the IOP8, the diabatic effects are predominant over the plain because the cooling of cold hydrometeors melting contributes to maintain the cold low-level air mass. The presence of this cold pool determines the limit of the moist easterly flow and then lets the down-valley flows extend over the plain. The comparison of wind direction (not shown) inside Toce valley ,at DOW location, for all the sensitivity experiments confirms that the diabatic effects give a temporal contribution to the down-valley flow shifting. This down-valley flow generally weak (less than 5 m s^{-1}) vanishes when the opposite flow reaches the orography.

5. CONCLUSION

The IOP3 and IOP8 are typical south-westerly situations where a northerly flow is observed at the foothills of the Alps.

The geographical origins of this northerly flow are identified: the three valleys (Toce, Ticino, Como valley) are cul-de-sac for the low-level southerly and easterly flow. The major contribution provides from both the Como valley and the Ticino valley for the IOP3 and from only the Toce valley for the IOP8. Nevertheless the intensity, the thickness and the duration of the IOP8 opposite flow is greater than the IOP3 one.

The different sensitivity experiments show that these two IOPs obey to two different conceptual schemes:

- in agreement with the conclusion of Steiner *et al.*2003 performed with radar and surface data, the reverse flow of IOP8 within the Toce valley mainly originates from diabatic effects i.e. the subsidence caused by melting of precipitation particles over the orography (more than 400 meters height).

  The reverse flow extension over the plain is mainly driven by the presence of the cold low-level air mass which protects the Alps foothills from the easterly low-level jet and the southerly moist low-level jet. The diabatic effects i.e. the cooling caused by melting of precipitation particles over the plain (less than 400 meters height) contribute to the maintain of this cold pool.

The northerly flow vanishes when the opposite easterly flow reaches the foothills and is strong enough to get up-valley flows.

- as illustrated in Brig meeting (Asencio et al,2003), the IOP3 reverse flow mainly originates from dynamical effects i.e. the upstream flow intensity and the transition from blocked to unblocked regime over the Alps. The wet drainage flow contribution is only concentrated on one hour delay for the beginning and the end of the reverse flow.

  The northerly flow vanishes when the mid-troposheric southerly wind is strong enough to pass over the Alps.

References

[1] N. Asencio, J. Stein M. Chong and F. Gheusi 2003 , Analysis of the northerly low-level flow in the Po Valley during the southwesterly MAP-IOP3., *Icam and map meeting 2003, brig, switzerland.* **A**, 16–19.

[2] P. Bechtold, E. Bazile, P. Mascart and E. Richard 2001 , A mass flux convection scheme for regional and global models, *Quart. j. roy. meteor. soc.* **127**, 869–886.

[3] O. Bousquet, F. Bradley , Smull 2003 , Observations and impacts of upstream blocking during a widespread orographic event, *Quart. j. roy. meteor. soc.* **129**, 391–410.

[4] C. Frei and E. Häller 2001 , Mesoscale precipitation analysis from MAP SOP rain-gauge data, *Map newsletter* **15**, 257–260.

[5] F. Gheusi and J. Stein 2002 , Lagrangian description of air flows using eulerian passive tracers, *Quart. j. roy. meteor. soc.* **128**, 337–360.

[6] C. Keil and C. Cardinali 2003 , The ECMWF Re-Analysis of the MAP SOP, *Internal report from ecmwf* **401**.

[7] J.P. Lafore, J. Stein, N. Asencio, Bougeault P. Ducrocq V. Duron J. Fischer C. Héreil P. Mascart P. Redelsperger J.L. Richard E. and J. Vilà-Guerau de Arellano 1998 , The Meso-NH atmospheric simulation system. Part I : Adiabatic formulation and control simulations, *Annales geophysicae* **16**, 90–109.

[8] R. Rotunno and R. Ferretti 2003 , Orographic effects on rainfall in MAP cases IOP2b and IOP8, *Quart. j. roy. meteor. soc.* **129**, 373–390.

[9] M. Steiner, O. Bousquet, O. Robert,A. Houze Jr. Bradley F. Smull Marco Mancini 2003 , Airflow within major Alpine river valleys under heavy rainfall, *Quart. j. roy. meteor. soc.* **129**, 411–432.